Inorg. Chem. **1990**, *29*, 3182-3187

Contribution from the Department of Chemistry, University of Arizona, Tucson, Arizona 85721,
and Anorganisch-Chemisches Institut der Technischen Universität München,
Lichtenbergstrasse 4, 8046 Garching, Federal Republic of Germany

Phosphorus-31 NMR Spectroscopy as a Probe of Models for the Molybdenum–Phosphate Interaction in "Oxo-Type" Molybdoenzymes and Their Cofactors

Ulrich Küsthardt,[1a,b] Michael J. LaBarre,[1a] and John H. Enemark*,[1a]

Received February 22, 1989

Six mononuclear oxomolybdenum(V) and dioxomolybdenum(VI) complexes containing the hydrotris(3,5-dimethyl-1-pyrazolyl)borate ligand and a catechol- or phenol-based ligand with a pendant phosphate ester have been prepared and characterized by physical methods. Molecular modeling calculations show that the nonbonded Mo···P distances are restricted to 4–8 Å, depending upon the stereochemical constraints of the ligands. ^{31}P NMR spectra of the Mo(V) complexes exhibit line broadening due to the d^1 Mo(V) center. The observed relaxation times (T_1 and T_2) are sensitive to the overall structure of the model compounds, and reasonable Mo···P distances can be calculated by using the Solomon equation.

Introduction

Molybdenum is an essential trace metal that is present in "oxo-type" enzymes such as xanthine oxidase (XO), sulfite oxidase (SO), and nitrate reductase (NR).[2-4] These enzymes occur in diverse organisms and catalyze reactions involving a change in the number of oxygen atoms in the substrate. From degradation studies, a common molybdenum cofactor (Mo-co) is proposed to be present in all these enzymes (Figure 1).[5,6] Further evidence for the terminal phosphate group on the side chain of the tetrahydropterin ring system of Mo-co comes from ^{31}P NMR studies on xanthine oxidase.[7] Oxidized XO shows a pH-dependent resonance at −3 ppm that can be assigned to the monosubstituted phosphate of Mo-co. Extensive broadening of this ^{31}P resonance occurs when oxidized XO is treated with dithionite and ethylene glycol to produce a stable inhibited Mo(V) form of the enzyme. This result is consistent with rapid relaxation of the ^{31}P nucleus by the paramagnetic molybdenum(V) center within ~10 Å. Several laboratories are engaged in research on molybdenum–thiolate,[8,9] molybdenum–thiolene,[8,9] and molybdenum–pterin[10] complexes. However, to date no model compounds have been available to allow examination of the possible molybdenum–phosphate interactions of Mo-co. Our approach has been to synthesize a series of stable mononuclear oxo-molybdenum(V) and dioxo-molybdenum(VI) complexes possessing pendant phosphate esters in which the Mo···P interactions are constrained to be 4–8 Å. The ^{31}P NMR spectra of these model compounds provide direct information about the effects of a paramagnetic oxo-molybdenum(V) center on the chemical shifts and line widths of nearby phosphate groups. Such information should ultimately be useful for using ^{31}P NMR to probe the Mo···P distance in solutions of the molybdenum cofactor. A preliminary account of this work has appeared.[11]

Experimental Section

General Techniques. Reactions were carried out under an atmosphere of pure dry nitrogen; solvents were thoroughly degassed and purified by distillation before use: tetrahydrofuran (thf) from potassium; dichloromethane and 1,2-dichloroethane from P_2O_5; acetonitrile from calcium hydride; toluene from sodium; hexanes from sodium hydride. Subsequent workup of the products was carried out in air. Silica gel 60 used in adsorption chromatography was obtained from Sigma Co. Potassium hydrotris(3,5-dimethyl-1-pyrazolyl)borate,[12] dichloro(hydrotris(3,5-dimethyl-1-pyrazolyl)borato)oxomolybdenum(V)[9c] ($LMoOCl_2$), and chloro(hydrotris(3,5-dimethyl-1-pyrazolyl)borato)dioxomolybdenum(VI)[13] ($LMoO_2Cl$) were prepared by literature methods. Triethylamine was purified by distillations from calcium hydride and potassium. Diphenyl chlorophosphate, 1,2,3-trihydroxybenzene, 1,2,4-benzenetriol, hydroquinone, and resorcinol were obtained from Aldrich Chemical Co. The purity of isolated compounds as well as the progress of the reactions were monitored by thin-layer chromatography. Analyses were performed by Atlantic Microlab Inc., Atlanta, GA, and by the Microanalytic Laboratories of the TU München, Garching, West Germany.

Preparation of $LMoO(O_2C_6H_3\text{-}3\text{-}OH)$ (1). To 2.0 g (4.2 mmol) of $LMoOCl_2$ (L = hydrotris(3,5-dimethyl-1-pyrazolyl)borate and 0.55 g (4.4 mmol) of 1,2,3-trihydroxybenzene in a 100-mL airless flask were added 50 mL of toluene and 0.9 mL of (excess) triethylamine. The reaction mixture was heated to 80 °C with vigorous stirring and held there for 1 h. The green solution was evaporated to dryness in vacuo and purified by adsorption chromatography on silica gel. Separation with 1,2-dichloroethane gave three fractions: light green starting material ($LMoOCl_2$), a dark green fraction, and finally olive green **1**. Recrystallization of **1** from dichloromethane/hexane mixtures gave dark olive green microcrystals. The yield was 1.03 g (46%).

Anal. Calcd for $C_{21}H_{26}N_6O_4BMo$ ($M_r = 533.23$): C, 47.30; H, 4.92; N, 15.76. Found: C, 47.14; H, 4.98; N, 15.70. IR (KBr): ν(MoO), 939 cm^{-1}; ν(OH), 3430 cm^{-1}. EPR (toluene; 296 K): $\langle g \rangle = 1.950$; $\langle A \rangle = 39.8 \times 10^{-4}$ cm^{-1}. UV–vis (1,2-dichloroethane; 20 °C): 14 990 cm^{-1} (190 L mol^{-1} cm^{-1}), 28 440 (4070). CV (vs Hg/Hg_2Cl_2): $E = -0.71$ V; $\Delta E_p = 65$ mV.

Preparation of $LMoO(O_2C_6H_3\text{-}4\text{-}OH)$ (3) was carried out as for **1** with 0.55 g (4.4 mmol) of 1,2,4-benzenetriol. The product was chromatographed on silica gel and eluted with dichloromethane as a light brown fraction. After recrystallization, golden-brown shiny plates were obtained. The yield was 1.76 g (79%). IR (KBr): ν(MoO), 938 cm^{-1}; ν(OH), 3390 cm^{-1}. EPR (toluene, 296 K): $\langle g \rangle = 1.949$; $\langle A \rangle = 38.1 \times 10^{-4}$ cm^{-1}. UV–vis (1,2-dichloromethane; 20 °C): 13 320 cm^{-1} (110 L mol^{-1} cm^{-1}), 31 610 (sh ~ 2490). CV (vs Hg/Hg_2Cl_2): $E = -0.76$ V; $\Delta E_p = 75$ mV.

Preparation of $LMoOCl(OC_6H_4\text{-}3\text{-}OH)$ (5). To 1.5 g (3.1 mmol) of $LMoOCl_2$ and 0.34 g (3.1 mmol) of resorcinol in a 100-mL airless flask were added 30 mL of toluene and 0.44 mL (3.1 mmol) of triethylamine. The reaction mixture was heated to 80 °C with vigorous stirring and held

---

(1) (a) University of Arizona. (b) Technische Universität München.

(2) (a) Rajagopalan, K. V. In *Biochemistry of the Essential Ultratrace Elements*; Frieden, E., Ed.; Plenum Press: New York, 1984; p 149. (b) Rajagopalan, K. V. *Nutr. Rev.* **1987**, *45*, 321. (c) Burgmayer, S. J. N.; Stiefel, E. I. *J. Chem. Educ.* **1985**, *62*, 943.

(3) Coughlan, M. P., Ed. *Molybdenum and Molybdenum Containing Enzymes*; Pergamon Press: New York, 1980.

(4) Spiro, T. G., Ed. *Molybdenum Enzymes*; J. Wiley: New York, 1985.

(5) (a) Johnson, J. L.; Hainline, B. E.; Rajagopalan, K. V. *J. Biol. Chem.* **1980**, *255*, 1783. (b) Johnson, J. L.; Hainline, B. E.; Rajagopalan, K. V.; Arison, B. H. *J. Biol. Chem.* **1984**, *259*, 5414.

(6) (a) Johnson, J. L.; Rajagopalan, K. V. *Proc. Natl. Acad. U.S.A.* **1982**, *79*, 6856. (b) Johnson, J. L. In ref 3, p 374.

(7) (a) Davis, M. D.; Edmondson, D. E.; Müller, F. *Eur. J. Biochem.* **1984**, *145*, 237. (b) Edmondson, D. E.; Davis, M. D.; Müller, F. In *Flavins and Flavoproteins*; Bray, R. C., Engel, P. C., Mayhew, S. G., Eds.; Walter de Gruyter: Berlin, 1984; p 309.

(8) (a) Garner, C. D.; Bristow, S. In ref 4, p 343. (b) Kaul, B. B.; Enemark, J. H.; Merbs, D. L.; Spence, J. T. *J. Am. Chem. Soc.* **1985**, *107*, 2885.

(9) (a) Holm, R. H. *Chem. Rev.* **1987**, *87*, 1401. (b) Stiefel, E. I. In *Comprehensive Coordination Chemistry*; Wilkinson, G., Ed.; Pergamon Press: Oxford, England, 1987; Vol. 3, p 1375. (c) Cleland, W. E., Jr.; Barnhart, K. M.; Yamanouchi, K.; Collison, D.; Mabbs, F. E.; Ortega, R. B.; Enemark, J. H. *Inorg. Chem.* **1987**, *26*, 1017.

(10) Burgmayer, S. J. N.; Stiefel, E. I. *J. Am. Chem. Soc.* **1986**, *108*, 8310.

(11) Küsthardt, U.; Enemark, J. H. *J. Am. Chem. Soc.* **1987**, *108*, 7926.

(12) Trofimenko, S. *J. Am. Chem. Soc.* **1967**, *85*, 6288.

(13) Roberts, S. A.; Young, C. G.; Kipke, C. A.; Cleland, W. E., Jr.; Yamanouchi, K.; Enemark, J. H. To be published.

0020-1669/90/1329-3182$02.50/0

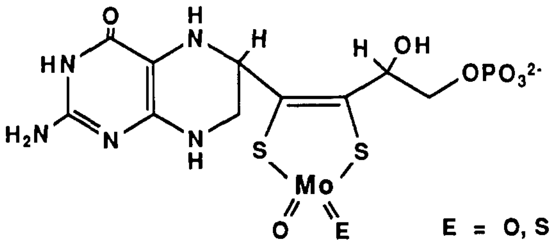

Figure 1. Molybdenum cofactor (Mo-co) present in XO, SO, and NR.

there for 30 min. The purple solution was evaporated to dryness in vacuo and purified by adsorption chromatography on silica gel. Separation with 1,2-dichloroethane yielded three fractions: light green starting material ($\mathrm{LMoOCl_2}$), a dark purple fraction, and finally purple **5**. Recrystallization from dichloromethane/hexane mixtures gave 0.52 g (30%) of dark purple microcrystals.

IR (KBr): ν(LMoCl), 335 cm^{-1}; ν(MoO), 949 cm^{-1}; ν(OH), 3440 cm^{-1}. EPR (toluene; 296 K): $\langle g \rangle = 1.938$; $\langle A \rangle = 44.7 \times 10^{-4}$ cm^{-1}. UV–vis (1,2-dichloroethane; 20 °C): 18 870 cm^{-1} (1320 L mol^{-1} cm^{-1}), 27 930 (2090).

Preparation of $\mathbf{LMoOCl(OC_6H_4\text{-}4\text{-}OH)}$ (7) was carried out as for **5** with 0.34 g (3.1 mmol) of hydroquinone, chromatographed on silica gel, and eluted with dichloromethane. Recrystallization from dichloromethane/hexane mixtures yielded 0.38 g (22%) of blue–gray microcrystals.

IR (KBr): ν(MoCl), 335 cm^{-1}; ν(MoO), 948 cm^{-1}; ν(OH), 3450 cm^{-1}. EPR (toluene; 296 K): $\langle g \rangle = 1.937$; $\langle A \rangle = 44.7 \times 10^{-4}$ cm^{-1}. UV–vis (1,2-dichloroethane; 20 °C): 16 950 cm^{-1} (960 L mol^{-1} cm^{-1}), 27 190 (sh ~ 3190). CV (vs $\mathrm{Hg/Hg_2Cl_2}$): $E = -0.69$ V; $\Delta E_p = 60$ mV.

Preparation of $\mathbf{LMoO_2(OC_6H_4\text{-}3\text{-}OH)}$ (9). To 0.5 g (1.1 mmol) of $\mathrm{LMoO_2Cl}$ and 0.25 g (2.3 mmol) of resorcinol in a 100-mL airless flask were added 30 mL of toluene and 0.3 mL (2.2 mmol) of triethylamine. The reaction mixture was refluxed for 5 h. The orange solution was evaporated to dryness in vacuo and purified by adsorption chromatography on silica gel. Elution with dichloromethane gave two organge fractions. The second dark orange fraction yielded, after recrystallization from dichloromethane/hexane mixtures, 0.4 g (69%) of orange needles of **9**.

IR (KBr): ν(MoO), 923 and 896 cm^{-1}; ν(OH), 3360 cm^{-1}. EPR: silent. ^{1}H NMR ($\mathrm{CD_2Cl_2}$; 20 °C): 2.30 (s, 6 H), 2.39 (s, 3 H), 2.40 (s, 6 H), 2.74 (s, 3 H), 5.84 (s, 2 H), 5.92 (s, 1 H), 6.42 (m, 2 H), 6.50 (m, 2 H), 7.10 ppm (m, 1 H).

Preparation of $\mathbf{LMoO_2(OC_6H_4\text{-}OH)}$ (11) was carried out as for **9** with 0.25 g (2.3 mmol) of hydroquinone, yielding 0.39 g (67%) of **11** as dark orange needles.

IR (KBr): ν(MoO), 924 and 894 cm^{-1}; ν(OH), 3395 cm^{-1}. EPR: silent. ^{1}H NMR ($\mathrm{CD_2Cl_2}$, 20 °C): 2.29 (s, 6 H), 2.36 (s, 3 H), 2.39 (s, 6 H), 2.77 (s, 3 H), 4.83 (s, 1 H), 5.82 (s, 2 H), 5.91 (s, 1 H), 6.78 ppm (m, 4 H). UV–vis (1,2-dichloroethane; 20 °C): 29 590 cm^{-1} (3760 L mol^{-1} cm^{-1}).

Preparation of $\mathbf{LMoO(O_2C_6H_3\text{-}3\text{-}OPO(OPh)_2)}$ (2). To 0.5 g (0.9 mmol) of $\mathrm{LMoO(O_2C_6H_3\text{-}3\text{-}OH)}$ (**1**) in a 50-mL airless flask were added 30 mL of toluene, 0.2 mL of (excess) triethylamine, and 0.5 mL (excess) of diphenyl chlorophosphate. The reaction mixture was refluxed for 15 h. The green solution was evaporated to dryness in vacuo and purified by adsorption chromatography on silica gel. Elution with dichloromethane and recrystallization from dichloromethane/hexane mixtures yielded 0.5 g (70%) of green microcrystals.

Anal. Calcd for $\mathrm{C_{33}H_{35}N_6O_7PBMo}$ ($M_r = 765.40$): C, 51.79; H, 4.61; N, 10.98. Found: C, 51.62, H, 4.61; N, 10.85. IR (KBr): ν(MoO), 942 cm^{-1}. EPR (toluene; 296 K): $\langle g \rangle = 1.949$; $\langle A \rangle = 39.2 \times 10^{-4}$ cm^{-1}. UV–vis (1,2-dichloroethane; 20 °C): 15 240 cm^{-1} (130 L mol^{-1} cm^{-1}), 29 410 (sh ~ 3360). CV (vs $\mathrm{Hg/Hg_2Cl_2}$): $E = -0.62$ V; $\Delta E_p = 65$ mV. ^{31}P NMR ($\mathrm{CHCl_3}$; 20 °C): −12.26 ppm (s); $\Delta\nu_{1/2} = 207$ Hz.

Preparation of $\mathbf{LMoO(O_2C_6H_4\text{-}4\text{-}OPO(OPh)_2)}$ (4) was carried out as for **2**, starting with 0.5 g (0.9 mmol) of **3** and yielded 0.26 g (89%) of **4** as green microcrystals. Anal. Calcd for $\mathrm{C_{33}H_{35}N_6O_7PBMo}$ ($M_r = 765.40$): C, 51.79; H, 4.61; N, 10.98. Found: C, 51.60; H, 4.70; N, 10.88. IR (KBr): ν(MoO), 940 cm^{-1}. EPR (toluene; 296 K): $\langle g \rangle = 1.948$; $\langle A \rangle = 38.2 \times 10^{-4}$ cm^{-1}. UV–vis (1,2-dichloroethane; 20 °C): 15 240 cm^{-1} (250 L mol^{-1} cm^{-1}), 28 090 (sh ~ 3200). CV (vs $\mathrm{Hg/Hg_2Cl_2}$): $E = -0.66$ V; $\Delta E_p = 70$ mV. ^{31}P NMR ($\mathrm{CHCl_3}$; 20 °C): −15.16 ppm (s); $\Delta\nu_{1/2} = 24$ Hz.

Preparation of $\mathbf{LMoOCl(OC_6H_4\text{-}3\text{-}OPO(OPh)_2)}$ (6) was carried out as for **2**, starting with 0.5 g (0.9 mmol) of **5** and yielding 0.51 g (72%) of **6** as red-purple microcrystals.

Anal. Calcd for $\mathrm{C_{33}H_{36}N_6O_6PBClMo}$ ($M_r = 785.86$): C, 50.44; H, 4.49; N, 10.69. Found: C, 50.59; H, 4.55; N; 10.70. IR (KBr): ν(MoCl), 336 cm^{-1}; ν(MoO), 950 cm^{-1}. EPR (toluene; 296 K): $\langle g \rangle = 1.939$; $\langle A \rangle = 44.4 \times 10^{-4}$ cm^{-1}. UV–vis (1,2-dichloroethane; 20 °C): 19 840 cm^{-1} (1440 L mol^{-1} cm^{-1}), 29 410 (2370). CV (vs $\mathrm{Hg/Hg_2Cl_2}$): $E = -0.51$ V; $\Delta E_p = 70$ mV. ^{31}P NMR ($\mathrm{CHCl_3}$; 20 °C): −17.08 ppm (s); $\Delta\nu_{1/2} = 15$ Hz.

Preparation of $\mathbf{LMoOCl(OC_6H_4\text{-}4\text{-}OPO(OPh)_2)}$ (8) was carried out as for **2**, starting with 0.5 g (0.9 mmol) of **7** and yielding 0.46 g (62%) of **8** as red-purple microcrystals.

Anal. Calcd for $\mathrm{C_{33}H_{36}N_6O_6PBClMo}$ ($M_r = 785.86$): C, 50.44; H, 4.49; N, 10.69. Found: C, 50.72; H, 4.78; N, 10.32. IR (KBr): ν(MoCl), 335 cm^{-1}; ν(MoO), 955 cm^{-1}. EPR (toluene; 296 K): $\langle g \rangle = 1.938$; $\langle A \rangle = 45.2 \times 10^{-4}$ cm^{-1}. UV–vis (1,2-dichloroethane; 20 °C): 19 310 cm^{-1} (1840 L mol^{-1} cm^{-1}), 25 710 (2370). CV (vs $\mathrm{Hg/Hg_2Cl_2}$): $E = -0.62$ V; $\Delta E_p = 70$ mV. ^{31}P NMR ($\mathrm{CHCl_3}$; 20 °C): −17.08 ppm (s); $\Delta\nu_{1/2} = 6$ Hz.

$\mathbf{LMoO_2(OC_6H_4\text{-}3\text{-}OPO(OPh)_2)}$ (10). To 0.25 g (0.5 mmol) of $\mathrm{LMoO_2(OC_6H_4\text{-}3\text{-}OH)}$ in 50-mL airless flask were added 20 mL of toluene, 0.1 mL (excess) of triethylamine, and 0.25 mL (excess) of diphenyl chlorophosphate. The reaction mixture was refluxed for 15 h. The orange solution was evaporated to dryness in vacuo and purified by adsorption chromatography on silica gel. Elution with 1,2-dichloroethane and recrystallization from dichloromethane/hexane mixtures yielded 0.31 g (86%) of orange microcrystals.

Anal. Calcd for $\mathrm{C_{33}H_{36}N_6O_7PBMo}$ ($M_r = 766.41$): C, 51.72; H, 4.74; N, 10.97. Found: C, 51.89; H, 4.96; N, 10.71. IR (KBr): ν(MoO), 922 and 896 cm^{-1}. EPR: silent. UV–vis (1,2-dichloroethane; 20 °C): 29 450 cm^{-1} (2230 L mol^{-1} cm^{-1}). ^{1}H NMR ($\mathrm{CD_2Cl_2}$; 20 °C): 2.30 (s, 6 H), 2.43 (s, 9 H), 2.77 (s, 3 H), 5.86 (s, 2 H), 5.96 (s, 1 H), 7.30 (m, 4 H), 7.40 ppm (m, 10 H). ^{31}*P NMR* ($\mathrm{CHCl_3}$; 20 °C): −17.62 ppm (s); $\Delta\nu_{1/2} = 4$ Hz.

Preparation of $\mathbf{LMoO_2(OC_6H_4\text{-}4\text{-}OPO(OPh)_2)}$ (12) was carried out as for **10**, starting with 0.25 g (0.5 mmol) of **11** and yielding 0.19 g (53%) of **12** as orange microcrystals.

Anal. Calcd for $\mathrm{C_{33}H_{36}N_6O_7PBMo}$ ($M_r = 766.41$): C, 51.72; H, 4.74; N, 10.97. Found: C, 51.65; H, 4.75; N, 10.96. IR (KBr): ν(MoO), 924 and 896 cm^{-1}. EPR: silent. UV–vis (1,2-dichloroethane; 20 °C): 29 330 cm^{-1} (2310 L mol^{-1} cm^{-1}). CV: irreversible reduction. ^{1}H NMR ($\mathrm{CD_2Cl_2}$; 20 °C): 2.28 (s, 6 H), 2.40 (s, 3 H), 2.41 (s, 6 H), 2.74 (s, 3 H), 5.84 (s, 2 H), 5.94 (s, 1 H), 6.89 (d, 2 H), 7.12 (d, 2 H), 7.23 (m, 6 H), 7.38 ppm (m, 4 H). ^{31}*P NMR* ($\mathrm{CHCl_3}$; 20 °C): −16.97 ppm (s); $\Delta\nu_{1/2} = 3$ Hz.

Physical Measurements. Infrared spectra were obtained as KBr pellets on a Perkin-Elmer PE983 spectrometer. Optical spectra were recorded on an IBM 9420 spectrophotometer. Electron paramagnetic resonance (EPR) spectra on fluid toluene solutions were measured at X-band frequencies by using a Varian E3 spectrometer. Cyclic voltammetric (CV) measurements were performed on acetonitrile solutions (1 mM) over the potential range +1.0 to −1.5 V (vs $\mathrm{Hg/Hg_2Cl_2}$) at a platinum-disk electrode on an IBM EC 225 voltammetric analyzer equipped with an IBM 742MT X-Y-T recorder. Nuclear magnetic resonance (NMR) spectra were obtained on Bruker WM-250 and AM-250 spectrometers. T_2 values were obtained through the relation $T_2 = (\pi(\Delta\nu_{1/2}))^{-1}$, where $\Delta\nu_{1/2}$ is the line width at peak half-height. T_1 values were obtained through the inversion recovery method on $\mathrm{CDCl_3}$ solutions (100 mM) at 20 °C.[14]

Molecular Modeling. The organic ligand fragments (e.g. "$\mathrm{O_2C_6H_3}$-3-$\mathrm{OPO(OPh)_2}$) were built up and the lowest energy van der Waals configuration determined by using CHEMX[15] on a MicroVAX-II computer. The structures of the metal-containing fragments ("LMoO" and "$\mathrm{LMoO_2}$") were derived from single-crystal structure data.[9c,16] The metal-containing fragments were then combined with the organic ligand fragments by using typical Mo–O single-bond distances (1.98 Å),[9b,17] and the range of sterically allowed Mo···P distances was investigated by using MMS[18] on a Silicon Graphics IRIS-2400 turbo computer.

Results and Discussion

Synthesis. A series of monooxomolybdenum(V) and dioxomolybdenum(VI) complexes possessing pendant phosphate esters attached to the metal via various catechol and phenol ligands can be prepared by straightforward two-step syntheses (Schemes

---

(14) Vold, R. L.; Waugh, Z. S.; Klein, M. P.; Phelps, D. E. *J. Chem. Phys.* **1968**, *48*, 3831.

(15) Chemical Design Ltd., Oxford, England 1986.

(16) Roberts, S. A.; Young, C. G.; Cleland, W. E., Jr.; Ortega, R. B.; Enemark, J. H. *Inorg. Chem.* **1988**, 27, 3044.

(17) Stiefel, E. I. *Prog. Inorg. Chem.* **1977**, *22*, 1.

(18) Molecular Modeling System. University of California, San Diego, 1986.

Scheme I

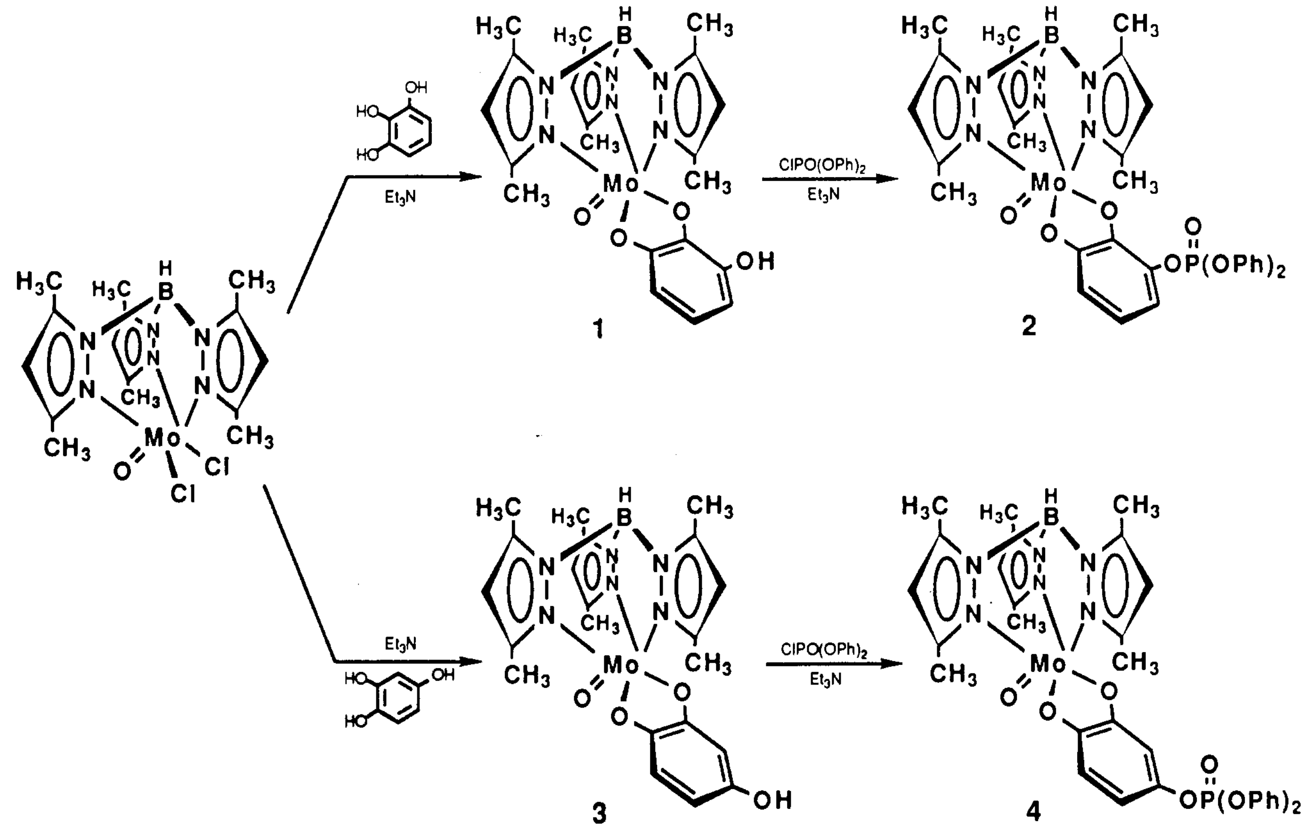

Scheme II

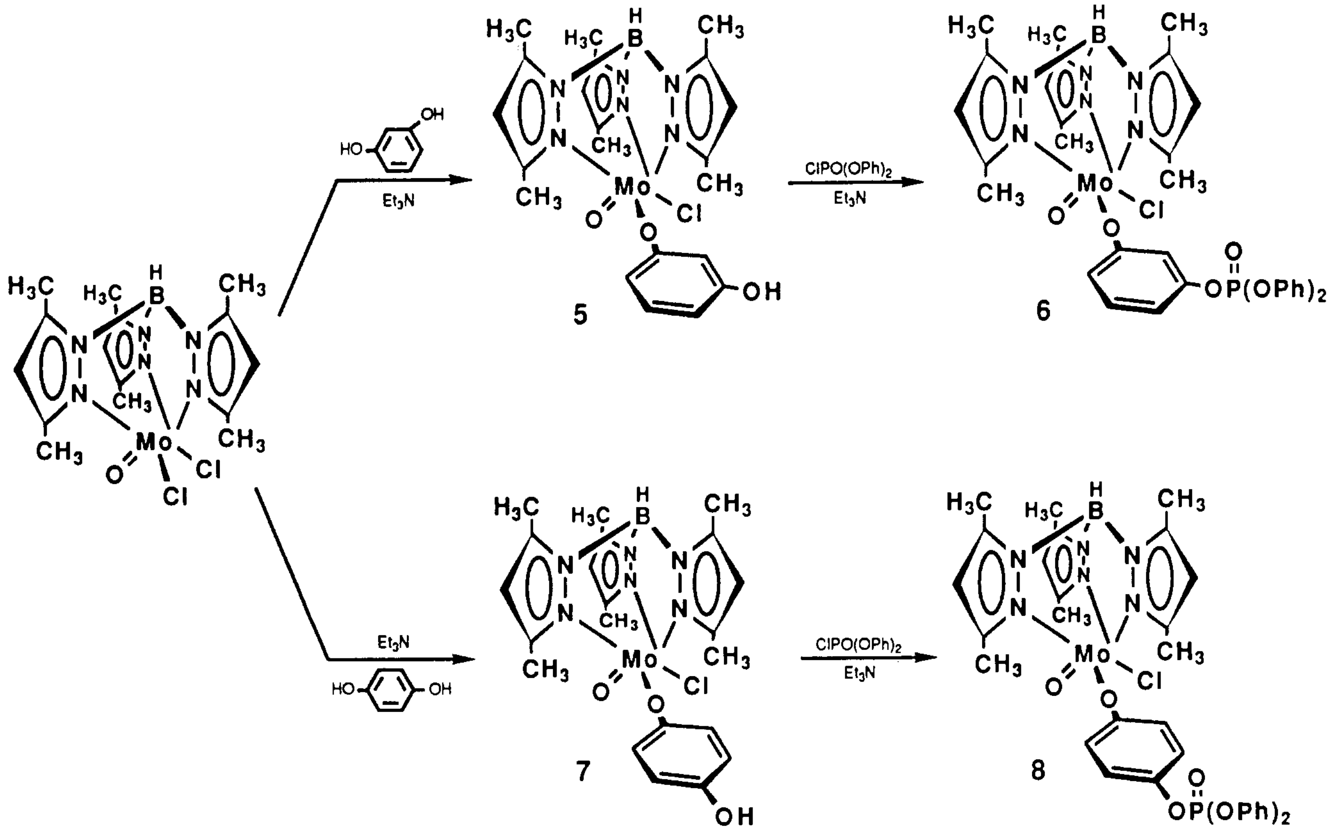

I–III). Common to all oxo–Mo(V) species is the precursor $LMoOCl_2$, which is synthesized by reaction of $MoCl_5$ in tetrahydrofuran with KL.[9c] The bidentate catechol precursors **1** and **3** are obtained from the reaction between $LMoOCl_2$ and the appropriate hydroxy-substituted catechols in the presence of 2 equiv of triethylamine in refluxing toluene (Scheme I). The monodentate phenol precursors **5** and **7** are formed in the reaction between $LMoOCl_2$ and the appropriate hydroxy-substituted (meta, para) phenols in the presence of 1 equiv of triethylamine (Scheme II). The common precursor for all dioxomolybdenum(VI) com-

Scheme III

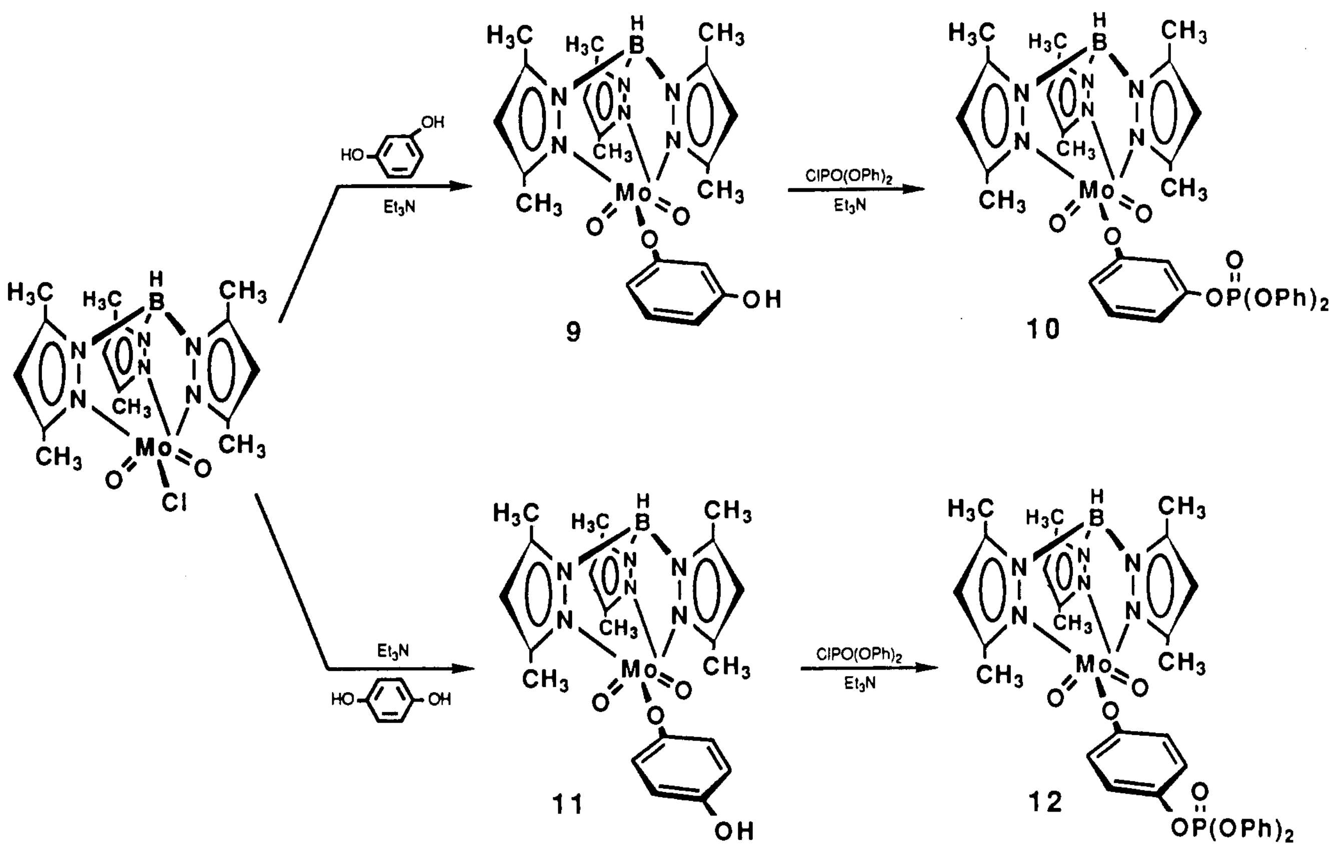

pounds is $LMoO_2Cl$, obtained from the reaction between MoO_2Cl_2 and KL.[13] The Mo(VI) complexes **9** and **11** (Scheme III) are prepared in a manner analogous to that used for **5** and **7**. Phosphorylation of the free hydroxyl group of **1**, **3**, **5**, **7**, **9**, and **11** with diphenyl chlorophosphate[19] in refluxing toluene in the presence of triethylamine provides the molybdenum phosphate ester complexes (Schemes I–III) in good yields.

Spectroscopic Properties. The EPR, IR, electronic, and electrochemical data of all mononuclear oxomolybdenum(V)–catechol complexes confirm the LMo(=O)(O,O) coordination sphere and exhibit values similar to those for the unsubstituted catechol complex, $LMoO(O_2iC_6H_4)$.[9c] The infrared spectra show the characteristic bands for the hydrotris(3,5-dimethyl-1-pyrazolyl)borate ligand and for metal–ligand vibrations and a strong band that can be assigned to the stretching vibration of the Mo=O group at about 940 cm^{-1}. The isotropic X-band fluid solution EPR spectra are typical for oxo–Mo(V) complexes.[9c] All of the substituted catechol complexes show very similar EPR parameters ($\langle g\rangle \cong 1.95$, $A(^{95,97}Mo) \cong 38 \times 10^{-4}$ cm^{-1}). For monooxomolybdenum(V) complexes of the type LMo(=O)(Cl)(O) the Mo=O stretching frequency is shifted by 5–10 cm^{-1} to higher wavenumbers, the $\langle g\rangle$ values are slightly lower ($\langle g\rangle \cong 1.94$), and the hyperfine splitting is substantially increased ($\langle A\rangle \cong 45 \times 10^{-4}$ cm^{-1}). All monooxo–Mo(V) compounds examined by cyclic voltammetry exhibit quasi-reversible one-electron reductions as demonstrated by $i_{pa}/i_{pc} \cong 1.0$, corresponding to formation of the analogous Mo(IV) monoanion (ΔE_p = 60–80 mV at a scan rate of 100 mV/s). The reduction potentials in acetonitrile range from −0.51 to −0.76 V (vs Hg/Hg_2Cl_2). The ^1H NMR spectra of the paramagnetic Mo(V) complexes give extremely broadened and slightly shifted signals that cannot be meaningfully interpreted.

The spectroscopic properties of the diamagnetic Mo(VI) complexes have characteristic features expected for a *cis*-$\{MoO_2\}^{2+}$ center. The vibrational spectra contain two Mo=O stretching modes separated by 25–30 cm^{-1} in the region 925–895 cm^{-1}. The electronic spectra of these d^0 complexes exhibit a single absorption maxima ($E_{max} \cong 29\,000$ cm^{-1}) that can be assigned to a ligand to metal charge-transfer electronic transition. The cyclic voltammograms exhibit irreversible reduction, as often occurs for dioxo–Mo(VI) complexes.[20]

The ^1H NMR spectra of the Mo(VI) complexes all show four resonances (integration: 6:3:6:3) for the methyl protons of the hydrotris(2,3-dimethyl-1-pyrazolyl)borate ligand due to the inequivalence of the methyl groups in the 3- and 5-positions and due to the local C_s symmetry. The C_s symmetry also causes the inequivalence of the three CH protons (integration: 2:1) of the pyrazolyl rings.

All attempts to obtain crystals of the molybdenum phosphate ester complexes suitable for X-ray structure determination have been unsuccessful, but we have done molecular modeling calculations in order to determine the possible Mo···P distances. The hydrotris(3,5-dimethyl-1-pyrazolyl)borate ligand imposes *fac* geometry at the metal center. The bulky methyl groups on the pyrazolylborate ligand and the phenyl groups on the phosphate ester severely restrict the rotational conformations of the pendant phosphate ester and thereby limit the Mo···P distances to the ranges given in Table I. For **2**, **4**, **6**, **8**, **10**, and **12**, the Mo···P distance is a function of the rotation of the phosphate ester about the C(cat)–O or C(phenol)–O bonds.

^{31}P NMR Studies. The ^{31}P NMR data for the phosphorylated compounds are shown in Table I. The ^{31}P resonances for **2** (−12.26 ppm), **4** (−15.16 ppm), and **6** (−10.31 ppm) are deshielded relative to triphenyl phosphate at −16.80 ppm. **8** possesses a slightly shielded ^{31}P resonance (−17.08 ppm). The ^{31}P signals of the diamagnetic Mo(VI) phosphate ester complexes (**10** and **12**) have chemical shifts of −17.62 and −16.97 ppm, respectively. Both are shielded relative to triphenyl phosphate and indicate the relatively small paramagnetic shift by the analogous Mo(V) compounds.

---

[19] Diethyl chlorophosphate can also be used, but the reaction time for the phosphorylation has be doubled to get satisfactory yields.

[20] Subramanian, P.; Spence, J. T.; Ortega, R. B.; Enemark, J. H. *Inorg. Chem.* **1984**, *23*, 2564.

Table I. ^{31}P NMR Data and Mo···P Distances of the Molybdenum Phosphate Ester Complexes

						d(Mo···P) [Å]		
complex	δ [ppm]	$\Delta\nu_{1/2}$ [Hz]	T_{2M} [s]^a	T_1 [s]^b	T_{1M} [s]^c	min^d	max^d	calc^e
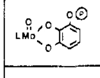 2	-12.26	207	0.0016	0.022	0.022	4.13	6.01	4.6
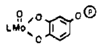 4	-15.16	24	0.0159	0.073	0.074	5.77	6.63	5.6
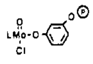 6	-10.31	15	0.0289	0.414	0.451	5.47	7.25	7.5
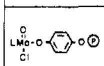 8	-17.08	6	0.159	0.423	0.458	6.74	7.55	7.6
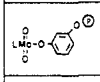 10	-17.62	4	—	5.09	—	—	—	—
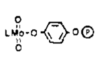 12	-16.97	3	—	—	—	—	—	—

^{a}Contribution of the unpaired electron nuclear coupling to the transverse relaxation time (calculated from $\Delta\nu_{1/2}$). ^{b}Measured by the inversion recovery method.[14] ^{c}Contribution of the unpaired electron nuclear coupling to the longitudinal relaxation time (calculated from T_1). ^{d}Obtained from molecular modeling calculations.[31] ^{e}Mo···P distance calculated from the Solomon–Bloembergen equation by using T_{1m} and $\tau_c = 4 \times 10^{-11}$ s.

The most striking feature of the ^{31}P NMR data for the Mo(V) models is the wide variation in their linewidths, which range from 207 Hz for **2** to 6 Hz for **8**. For comparison, the ^{31}P NMR resonances of the diamagnetic Mo(VI) compounds have line widths less than 4 Hz. The line broadening observed for the ^{31}P signals in the Mo(V) phosphate ester complexes is primarily due to coupling of the ^{31}P nucleus with the unpaired electron on the d^1 molybdenum centers.

The longitudinal relaxation times (T_1) were measured for the model compounds by the spin inversion recovery method.[21] The paramagnetic Mo(V) phosphate esters all have T_1 values less than 0.5 s, which vary by more than a factor of 10, whereas the Mo(VI) analogue has a much longer T_1 value of 5.09 s. The T_1 values for the Mo(V) complexes are much longer than their corresponding T_2 rates (as measured by $T_2^{-1} = \pi(\Delta\nu)$). Other ^{31}P studies have noted that T_2 rates are much faster than the T_1 values for phosphate groups in paramagnetic complexes.[22,23] Both T_1 and T_2 contain dipolar terms due to coupling between the metal ion unpaired electron and the ^{31}P nucleus. Since T_2 is so much smaller than T_1, it follows that dipolar mechanisms cannot be solely responsible for T_2, and therefore, T_1 values will be used for calculations where strictly dipole–dipole interactions are described.

The T_1 values can be used to calculate the Mo···P distance, r, through the Solomon equation (eq 1),[24,25] where μ_0 is the

$$T_1^{-1} = \frac{2}{15}\frac{(\mu_0)^2}{(\pi)^2}\frac{\delta_n^2 g_e^2 \mu_B^2 S(S+1)}{r^6}\left[\frac{7\tau_c}{1+\omega_s^2\tau_c^2}+\frac{3\tau_c}{1+\omega_I^2\tau_c^2}\right] \quad (1)$$

permeability of a vacuum, r is the distance between the nuclei, δ_n is the nuclear magnetogyric ratio, g_e is the electron g value, μ_B is the Bohr magneton, S is the spin quantum number, τ_c is the correlation time, and ω_s and ω_I are the electronic and nuclear angular velocities, respectively.[26] This equation has been shown to be valid for many instances[22-24] although problems may arise for small molecules in the assumption of point–point dipoles implicit in eq 1 due to electron density residing at or induced in pendant ligand positions by the nearby unpaired spin density at the metal.[27]

The correlation time, τ_c, for the Mo···P interaction in the Mo(V) phosphate compounds is assumed to be essentially constant because of their similar structures. A τ_c value of about 4×10^{-11} s is consistent with the Mo–P distances derived from the molecular modeling calculations and with the measured T_1 values. An independent estimate of τ_c can be obtained from summing the individual contributing terms (eq 2), where τ_s is the electronic

$$\tau_c^{-1} = \tau_s^{-1} + \tau_r^{-1} + \tau_m^{-1} \quad (2)$$

relaxation rate, τ_r is the rotational correlation time, and τ_m is the chemical exchange rate. There is no evidence for chemical exchange in these systems, so τ_m^{-1} is assumed to be 0. The rotational correlation time can be estimated from the Stokes–Einstein equation to be around 5×10^{-10} s, and the electronic relaxation rate is calculated to be about 10^{-8} or 10^{-9} s on the basis of EPR experiments.[28] These estimates yield a value of τ_c that is 1 or 2 orders of magnitude slower than the correlation time required by T_1 data and computer modeling. Experimental evidence shows that Stokes–Einstein estimations of τ_r can be ~5 times slower than actual measured rotational correlation times for phosphate groups bound to RNA polymerase with Mn(II).[22] Theoretical evidence also indicates that internal motions of the phosphate group in such complexes may mix with molecular rotational motion to significantly shorten correlation times.[29,30] The T_1:T_2 ratio suggests that internal motion of the phosphate group may also make a major contribution to τ_c in the present study to give an effective τ_c of 4×10^{-11}.

Conclusions

The utility of paramagnetic metal centers in NMR studies of coordination compounds and macromolecules has been well demonstrated.[22] Most studies have investigated the perturbations of the ^1H resonances by a paramagnetic center. There have been relatively few NMR studies of paramagnetic molecules in which ^{31}P is the probe nucleus.[31] Even more rare is the use of oxo–Mo(V) as the paramagnetic center for NMR relaxation studies. The above ^{31}P NMR results for several oxo–Mo(V) complexes containing pendant phosphate esters demonstrate that such systems can provide important structural information, in spite of the relatively long electronic relaxation times[27] and aspherical electronic distributions of oxo–Mo(V) complexes.[9c] This study of molybdenum–phosphate ester complexes by ^{31}P NMR is a first step toward similar investigations of other model systems and of the molybdenum cofactor of enzymes. Our results show that ^{31}P chemical shifts and relaxation times are sensitive to the overall structure of the model compounds and that reasonable Mo···P distances can be calculated from the longitudinal relation times by using the Solomon equation.[25] Molecular modeling calculations on the molybdenum cofactor show that it is possible that at some point in the catalytic cycle of the enzyme the phosphate group of the cofactor may actually occupy one of the coordination sites of the molybdenum atom. However, a definitive understanding of the molybdenum–phosphate interactions in "oxo-type" molybdoenzymes will require ^{31}P NMR relaxation data for the Mo(V)

---

(21) The ^{31}P NMR spectral data for the compounds in Table I have been verified by duplicate measurements on independently synthesized samples. However, it has not been possible to reproduce the results that we originally reported[11] for LMoO($C_6H_3CH(Me)OPO(OPh)_2$), and the weak ^{31}P signal previously observed near −5 ppm is now unassigned.

(22) Bean, B. L.; Koren, R.; Mildvan, A. S. *Biochemistry* **1977**, *16*, 3323.

(23) Mota de Freitas, D.; Luchinat, C.; Banci, L.; Bertini, I.; Valentine, J. S. *Inorg. Chem.* **1987**, *26*, 2788.

(24) Bertini, I.; Luchinat, C. In *NMR of Paramagnetic Molecules in Biological Systems*; The Benjamin/Cummings Publishing Co.: Menlo Park, CA, 1986.

(25) (a) Solomon, I. *Phys. Rev.* **1955**, *99*, 559.

(26) At the field used in these experiments, 5.875 T, ω_I (^{31}P) is ~6.36×10^8 rad/s and ω_s (e^-) is ~1.04×10^{12} rad/s.

(27) Gottlieb, H. P. W.; Barfield, M.; Doddrell, D. M. *J. Chem. Phys.* **1977**, *67*, 3785.

(28) The EPR line widths of **6**, **8**, **11**, and related compounds give $\tau_s = 10^{-8}$–10^{-9} s.

(29) Lipari, G.; Szabo, A. *J. Am. Chem. Soc.* **1982**, *104*, 4546.

(30) Lipari, G.; Szabo, A. *J. Am. Chem. Soc.* **1982**, *104*, 4559.

(31) Bertini, I.; Luchinat, C.; Scozzafara, A. *FEBS Lett.* **1978**, *93*, 251.

(32) Küsthardt, U. Unpublished results.

states of the enzymes and the synthesis and physical characterization of more sophisticated model compounds.

Acknowledgment. We thank Drs. G. Backes and K. Christensen for assistance with the ^{31}P NMR measurements and Dr. W. E. Cleland, Jr., for preliminary experiments and helpful discussions. We gratefully acknowledge financial support from the National Institutes of Health (Grant GM-37773) and thank the Alexander von Humboldt-Stiftung and the Fonds der Chemischen Industrie for fellowships to Dr. U. Küsthardt. We are grateful to a reviewer for several helpful comments and to Professor M. Barfield for useful discussions.

Contribution from the Department of Chemistry and Laboratory for Molecular Structure and Bonding,
Texas A&M University, College Station, Texas 77843

Electronic Structure Study of Dinuclear Transition-Metal Complexes with Alkynes as Bridges

F. Albert Cotton* and Xuejun Feng

Received August 1, 1989

Electronic structures of dinuclear complexes of Nb, Mo, Ta, and W with alkyne bridges are studied by way of molecular orbital calculations on model systems employing the SCF–Xα–SW method. It is shown that the large deviation of some of the alkyne bridges from a perpendicular orientation to the M–M bond, as in $Nb_2Cl_4O(PhCCPh)(THF)_4$, is caused electronically by second-order Jahn–Teller distortion. Comparison is made with the distortion in $W_2Cl_4(NMe_2)_2(\mu\text{-}MeCCMe)(py)_2$. The calculated results for $[Mo_2(\mu\text{-}4\text{-}MeC_6H_4CCH)(\mu\text{-}O_2CMe)(en)_4]^{3+}$ and $Ta_2Cl_6(Me_3CCCCMe_3)(THF)_2$ also show good agreement with the observed structural features. Similarities and differences in the electronic structures of different complexes are also discussed in detail, and the expected presence or absence of a second-order Jahn–Teller effect is shown to be the general key to understanding the structures.

Introduction

Synthetic study of the reactions of alkynes with transition-metal complexes has led to a large number of dinuclear complexes in which the alkyne acts as a bridge between the metal atoms.[1] All such complexes may be classified by the angle between the projections of the alkyne C–C bond and the M–M bond on a plane parallel to both. In some cases, the angle is about 180°, that is, the C–C vector is nearly parallel to the M–M vector, while in others the angle is around 90°, and the two vectors projected on the plane are nearly perpendicular. The electronic structures of both these types have been discussed in terms of a general molecular orbital analysis based on calculations by the extended Hückel method.[1]

However, recent studies have revealed that the alkyne bridge across the M–M bond may be far from either parallel or perpendicular. The first such example was the $W_2Cl_4(NMe_2)_2(\mu\text{-}MeCCMe)(py)_2$ molecule, reported by Chisholm and co-workers.[2] In this molecule the projected angle has a value of 55°, and thus the orientation of the C–C bond to the W–W bond is twisted from the perpendicular direction by 35°. Since the twisting apparently cannot be ascribed to steric factors, Calhorda and Hoffmann[3] did electronic structure studies employing model systems and extended Hückel calculations. They came to the conclusion that the actual geometry could be attributed to second-order Jahn–Teller distortion from a truly perpendicular geometry.

In this laboratory, we have reported very recently a new dinuclear complex of niobium with diphenylacetylene.[4] The molecule, $Nb_2Cl_4O(PhCCPh)(THF)_4$, has an unusual feature very similar to that found in the ditungsten case. The C–C bond is again twisted from the perpendicular orientation, this time by 31°. Once again, this large deviation cannot be explained by steric effects. On the other hand, the electronic structure obtained for the models of $W_2Cl_4(NMe_2)_2(\mu\text{-}MeCCMe)(py)_2$ may not be simply and directly used for understanding the present situation. The metal atoms in the two compounds have the same formal oxidation state, but the $(Nb_2)^{6+}$ unit has two electrons less than the $(W_2)^{6+}$ unit. Moreover, the ligand arrangement about the metal dimer in $Nb_2Cl_4O(PhCCPh)(THF)_4$ is different from that in $W_2Cl_4(NMe_2)_2(\mu\text{-}MeCCMe)(py)_2$. Thus it could well be that the explanation pertinent in the tungsten case is not appropriate for the niobium compound. Or, again, it might be true that the same final situation leading to a second-order Jahn–Teller distortion does arise both times, despite the differences in electron count and structure.

To understand the deviation of the PhCCPh molecule from the perpendicular orientation to the Nb–Nb bond in our case, we have carried out SCF–Xα–SW molecular orbital calculations on $Nb_2Cl_4O(PhCCPh)(THF)_4$. The results are reported in this paper together with electronic structure studies for two other complexes, namely, $[Mo_2(\mu\text{-}4\text{-}MeC_6H_4CCH)(\mu\text{-}O_2CMe)(en)_4]^{3+}$[5] and $Ta_2Cl_6(Me_3CCCCMe_3)(THF)_2$,[6] both having alkyne bridges over the metal–metal bonds. The ligand coordination in the molybdenum compound is similar to that in our niobium molecule, but the C–C and Mo–Mo vectors are almost perpendicular. The structure in the tantalum compound, on the other hand, is very similar to that in the ditungsten case, but the deviation is much smaller. As will be seen, a comparative study of the electronic structures of these molecules is more informative for understanding their molecular structural features than the results for any one individual molecule.

Computational Procedures

The SCF–Xα–SW[7] method was employed for the electronic structure calculations of the model systems (see Figure 1) of $Nb_2Cl_4O(PhCCPh)(THF)_4$, $[Mo_2(\mu\text{-}4\text{-}MeC_6H_4CCH)(\mu\text{-}O_2CMe)(en)_4]^{3+}$ (en = ethylenediamine), $Ta_2Cl_6(Me_3CCCCMe_3)(THF)_2$, and $W_2Cl_4(NMe_2)_2(\mu\text{-}MeCCMe)(py)_2$. In each case, the bridging RCCR molecules were modeled by HCCH. The THF groups, on the other hand, were replaced by H_2O.

For $Nb_2Cl_4O(PhCCPh)(THF)_4$, two model molecules were used for the calculations. The first model, $Nb_2Cl_4O(HCCH)(H_2O)_4$, adopted the geometry of the real molecule and has C_2 symmetry. It was calculated for two orientations of the C–C bond, namely, perpendicular to the Nb–Nb bond and rotated from that by 31.4°. The second model, $[Nb_2Cl_6O(HCCH)(H_2O)_2]^{2-}$, is different from the first one by replacing

---

(1) Hoffman, D. M.; Hoffmann, R.; Fisel, C. R. *J. Am. Chem. Soc.* **1982**, *104*, 3858. This paper contains a selected list of such complexes.

(2) Ahmed, K. J.; Chisholm, M. H.; Folting, K.; Huffman, J. C. *Organometallics* **1986**, *5*, 2171.

(3) Calhorda, M. J.; Hoffmann, R. *Organometallics* **1986**, *5*, 2187.

(4) Cotton, F. A.; Shang, M. *Inorg. Chem.* **1990**, *29*, 508.

(5) Kerby, M. C.; Eichhorn, B. W.; Vollhardt, K. P. C.; submitted to *J. Am. Chem. Soc.*

(6) Cotton, F. A.; Hall, W. *Inorg. Chem.* **1980**, *19*, 2354.

(7) Slater, J. C. *Quantum Theory of Molecules and Solids*; McGraw Hill: New York, 1974; Vol. IV.